Anthropogenic eutrophication of Lake Titicaca (Bolivia) revealed by carbon and nitrogen stable isotopes fingerprinting

C. Heredia, S. Guédron, D. Point, V. Perrot, S. Campillo, C. Verin, M.E. Espinoza, P. Fernandez, C. Duwig, D. Achá

Anthropogenic eutrophication of Lake Titicaca (Bolivia) revealed by carbon and nitrogen stable isotopes fingerprinting

C. Heredia[a,b*], S. Guédron[a,c], D. Point[b,d] , V. Perrot[a], S. Campillo[a], C. Verin[a], M.E. Espinoza[b], P. Fernandez[b], C. Duwig[c,e], and D. Achá[b]

[a]Université Grenoble Alpes, Université Savoie Mont Blanc, CNRS, IRD, IFSTAR, ISTerre, 38000, Grenoble, France.

[b]Instituto de Ecología, Unidad de Calidad Ambiental (UCA), Carrera de Biología, Universidad Mayor de San Andrés, Campus Universitario de Cota Cota, casilla 3161, La Paz, Bolivia.

[c]Laboratorio de Hidroquímica - Instituto de Investigaciones Químicas - Universidad Mayor de San Andrés, Campus Universitario de Cota-Cota, casilla 3161, La Paz, Bolivia.

[d] Géosciences Environnement Toulouse (GET) - Institut de Recherche pour le Développement (IRD), CNRS, Université de Toulouse.

[e]Univ. Grenoble Alpes, Univ. Savoie Mont Blanc, CNRS, IRD, IFSTTAR, IGE, 38000 Grenoble, France.

*Corresponding author:

Carlos Heredia A.; carlos.heredia-aguilar@univ-grenoble-alpes.fr

Highlights

- C and N stable isotopes were measured in four compartments of Lake Titicaca
- Anthropogenic discharge affects baseline C and N isotope signatures
- C recycling from soil, anthropogenic and lacustrine sources affect the $\delta^{13}C$ signature
- $\delta^{15}N$ signatures track anthropogenic contamination independently of plant type
- Decreased anthropogenic contribution in the bay assessed by isotope mixing model

Graphical abstract

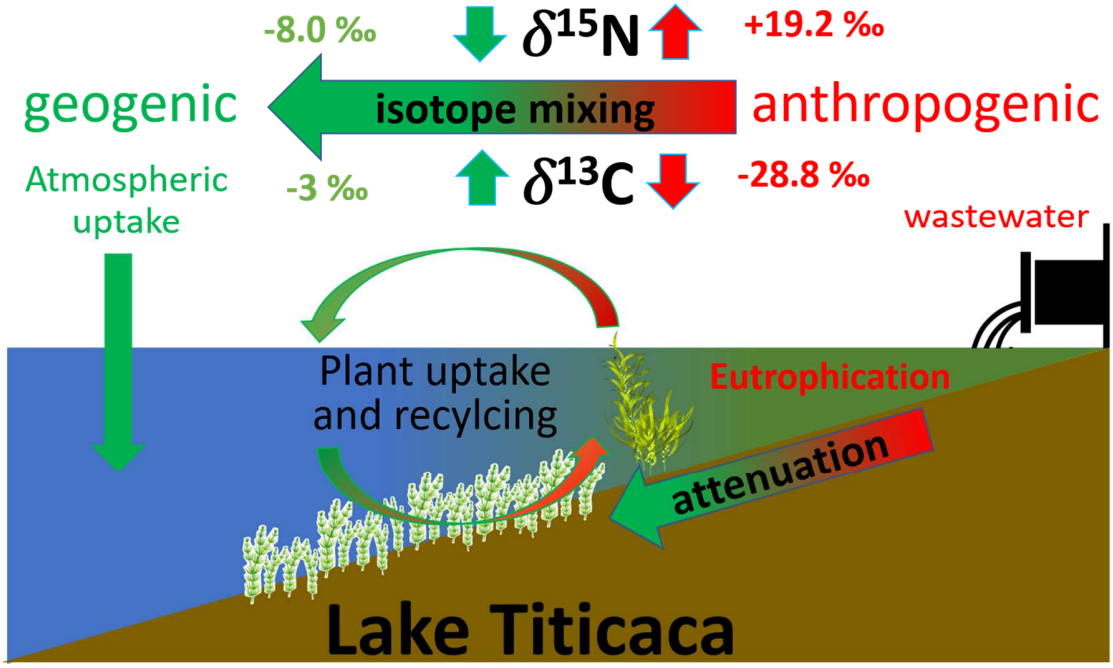

Abstract

Cultural eutrophication is the leading cause of water quality degradation worldwide. The traditional monitoring of eutrophication is time-consuming and not integrative in space and time. Here, we examined the use of carbon ($\delta^{13}C$) and nitrogen ($\delta^{15}N$) isotopic composition to track the degree of eutrophication in a bay of Lake Titicaca impacted by anthropogenic (urban, industrial and agricultural wastewater) discharges. Our results show increasing $\delta^{13}C$ and decreasing $\delta^{15}N$ signatures in macrophytes and suspended particulate matter with distance to the wastewater source. In contrast to $\delta^{15}N$ and $\delta^{13}C$ signatures, in-between aquatic plants distributed along the slope were not only affected by anthropogenic discharges but also by the pathway of carbon uptake, i.e., atmospheric (emerged) vs aquatic (submerged). A binary mixing model elaborated from pristine and anthropogenic isotope end-members allowed the assessment of anthropogenically derived C and N incorporation in macrophytes with distance to the source. Higher anthropogenic contribution was observed during the wet season, attributed to enhanced wastewater discharges and leaching of agricultural areas. For both seasons, eutrophication was however found naturally attenuated within 6 to 8 kilometers from the wastewater source. Here, we confirm that carbon and nitrogen stable isotopes are simple, integrative and time-saving tools to evaluate the degree of eutrophication (seasonally or annually) in anthropogenically impacted aquatic ecosystems.

Keywords: carbon stable isotopes, nitrogen stable isotopes, eutrophication, Lake Titicaca, anthropogenic discharges

1. Introduction

Human-induced eutrophication of surface waters has become a major concern of water quality impairment (Smith, 2003; Schindler, 2006). It is known to impact aquatic ecosystems (Backer and McGillicuddy Jr, 2006; Paerl and Otten, 2013) with environmental and health-related costs estimated to several billions of dollars per year (Pretty et al., 2003; Dodds et al., 2009). The discharge of untreated wastewater in natural aquatic ecosystems induces a nutrient enrichment in the water column, affecting the trophic structure and composition of the in biological communities (Smith et al., 2006). A common response to the excess of nutrient inputs is the possible development of massive algal proliferation (i.e., blooms) which provokes oxygen depletion (i.e., hypoxia or anoxia) during the bacterial degradation of senescent blooms that can result in the death of benthic and pelagic biota (Diaz, 2001). Recurrence of such hypoxic events can cause the release of phosphorus from sediments (due to changing redox conditions), creating an internal feedback that amplifies eutrophication effects (Rosenmeier et al., 2004; Vahtera et al., 2007; Smith et al., 2015).

The monitoring of eutrophication generally includes cost and time-consuming *in situ* physicochemical analyses (pH, redox potential, total nutrient concentration, biochemical oxygen demand, etc…) as well as macrophyte and algal species composition and biomass (Le Moal et al., 2018). In impermanently eutrophic ecosystems or those subject to occasional blooms, such traditional monitoring methods require a large number of measurements to obtain a significant spatial overview of the anthropogenic impacts, which are generally not constrained temporally. Therefore, the need for a different approach with sensitive techniques, providing a spatially and temporally integrative picture of eutrophication processes, is of high priority to understand the dissemination and triggering mechanisms of blooms. This latter

information is key for the development of mitigation strategies before irreversible changes affect aquatic ecosystems.

Carbon ($\delta^{13}C$) and nitrogen ($\delta^{15}N$) stable isotope are good candidates to provide such level of information at the ecosystem scale (Fry, 2006; Dawson and Siegwolf, 2007; Glibert et al., 2018). Both C and N isotopic tracers provide information about the food web structures and are influenced by baseline changes and sources (Vander Zanden and Rasmussen, 1999; Liu et al., 2012). $\delta^{13}C$ allows the inference of energy sources (i.e., no significant fractionation of C isotopes during trophic transfer, resulting in isotopic ratios between consumers and their food almost identical), whereas $\delta^{15}N$ allows the determination of trophic levels (i.e., enrichment factor between consumers and their food is between 2 and 4 ‰) (Dawson et al., 2002; Michener and Lajtha, 2008; Middelburg, 2014). In addition, when a significant difference in isotopic signatures exists between natural and anthropogenic sources, it is possible to track and assess the magnitude of anthropogenic pollution (Glibert et al., 2018). On the one hand, carbon stable isotope ratios ($\delta^{13}C_{org}$) can be used in freshwater ecosystems to distinguish between autochthonous and allochthonous sources of organic matter (Gu et al., 2006; Thevenon et al., 2012). $\delta^{13}C_{org}$ values of terrestrial primary productivity often differ from the $\delta^{13}C_{org}$ values of aquatic primary productivity (Fry, 2006). On the other hand, nitrogen stable isotope ratios ($\delta^{15}N$) can track anthropogenic nitrogen inputs (Glibert et al., 2018). The three primary sources of anthropogenically derived N in freshwater ecosystems are human and animal (e.g. septic and manure waste) sewage , synthetic fertilizers (from agricultural fields) and atmospheric deposition (Cole et al., 2006), with each of these sources often differing in their $\delta^{15}N$ signature. Sewage-derived N commonly presents $\delta^{15}N$ values enriched in heavier isotopes [≥10 ‰,)] relative to the baseline value of atmospheric deposition (N_2), which is closer to 0 (Kendall et al., 2008; Holtgrieve et al., 2011). Once discharged in surface or ground water,

anthropogenic N recycling (i.e., nitrification or denitrification) can cause large N isotope fractionation up to ±20 ‰ (Mariotti et al., 1988; Sebilo et al., 2003; Kendall et al., 2007). Changes in the isotopic composition of dissolved inorganic pools are reflected in the $\delta^{13}C_{org}$ and $\delta^{15}N$ of primary producers, which can assimilate dissolved nutrients from the water column and integrate the changes in isotopic sources over time (Schindler et al., 1997; Savage, 2005; Dawson and Siegwolf, 2007). Consequently, the $\delta^{13}C$ and $\delta^{15}N$ values of primary producers can alert the presence of anthropogenic nutrients before significant ecological changes occur in the environment (McClelland et al., 1997; Savage, 2005; Vermeulen et al., 2011). Enriched or depleted isotope ratios in relation to a "pristine" baseline can therefore be used as sensitive indicators of pollution (Costanzo et al., 2001).

In many developing countries, the demographic expansion and the development of urban centers and economic activities (e.g., mining, agriculture, industry) increase anthropogenic impacts on their surrounding ecosystems. This has been the case during the last few decades in the high-altitude Andean Altiplano (Mazurek, 2012), where the discharge of untreated wastewater from cities like Puno, Oruro, and La Paz/El Alto have led to the degradation of several water bodies. The most dramatic examples are the case of Lake Uru-Uru (Bolivia) (Alanoca et al., 2016; Guédron et al., 2017; Sarret et al., 2019), Puno Bay (Peru) in the northern basin of Lake Titicaca (Northcote, 1992), and Cohana Bay (Bolivia) in the southern basin of the Lake (Archundia et al., 2017a; Flores Avilés et al., 2022). Besides the permanent state of eutrophication in several shallow basins receiving untreated wastewater, punctual and sometimes massive bloom events have been reported at larger scales. For example, in 2015, Lake Titicaca suffered one of its major bloom event to date at the scale of its entire southern basin, triggered by an unusually intense rain episode that washed out large amounts of

nutrients from the agricultural watershed and resulted in the massive death of birds and pelagic biota (Achá et al., 2018).

In this study, we examined $\delta^{13}C$ and $\delta^{15}N$ signatures in primary producers (macrophytes, periphyton), suspended particulate matter, and surface sediments along an eutrophication gradient in Lake Titicaca. The aim of this study is to test the efficiency of these tools for monitoring the dissemination and amplitude of anthropogenic discharges of wastewaters while considering the natural functioning of the ecosystem (trophic status and seasonality).

2. Material and Methods

2.1. Study area

Lake Titicaca is the largest freshwater lake in South America. Located in the high tropical Andes (3809 m.a.s.l.) between Peru and Bolivia, it is divided into two separated basins: the northern great lake, namely Lago Mayor (7131 km^2; mean depth = 100 m; max depth = 285 m), and the southern small lake, namely Lago Menor (1428 km^2; mean depth = 10 m; max depth = 40 m) (**Fig. 1a**). Both basins are connected through the Strait of Tiquina (approx. 800 meters wide). The only outlet of the system, the Desaguadero River, is located in the southern end of Lago Menor (Dejoux and Iltis, 1991). Its high elevation results in extreme hydro-climatic conditions, e.g., intense UV-radiation (Richerson et al., 1986; Villafae et al., 1999), lower dissolved oxygen (Achá et al., 2018), and large daily temperature variations which can overwhelm seasonal ones (Molina et al., 2014).

The climate of the Titicaca region is marked by a seasonal cycle of precipitation, and more than 70% of the precipitation occurs during the austral summer (mean annual precipitation ~614 mm $year^{-1}$), concentrated between December and March, when moist air from the

Amazon enters the Altiplano and discharges in the form of convective rainfalls (Guédron et al., 2018; Segura et al., 2019). Precipitation during the Austral summer produces intense and short duration floods of the lake's tributaries on the steep slopes of the lake (Roche et al., 1992).

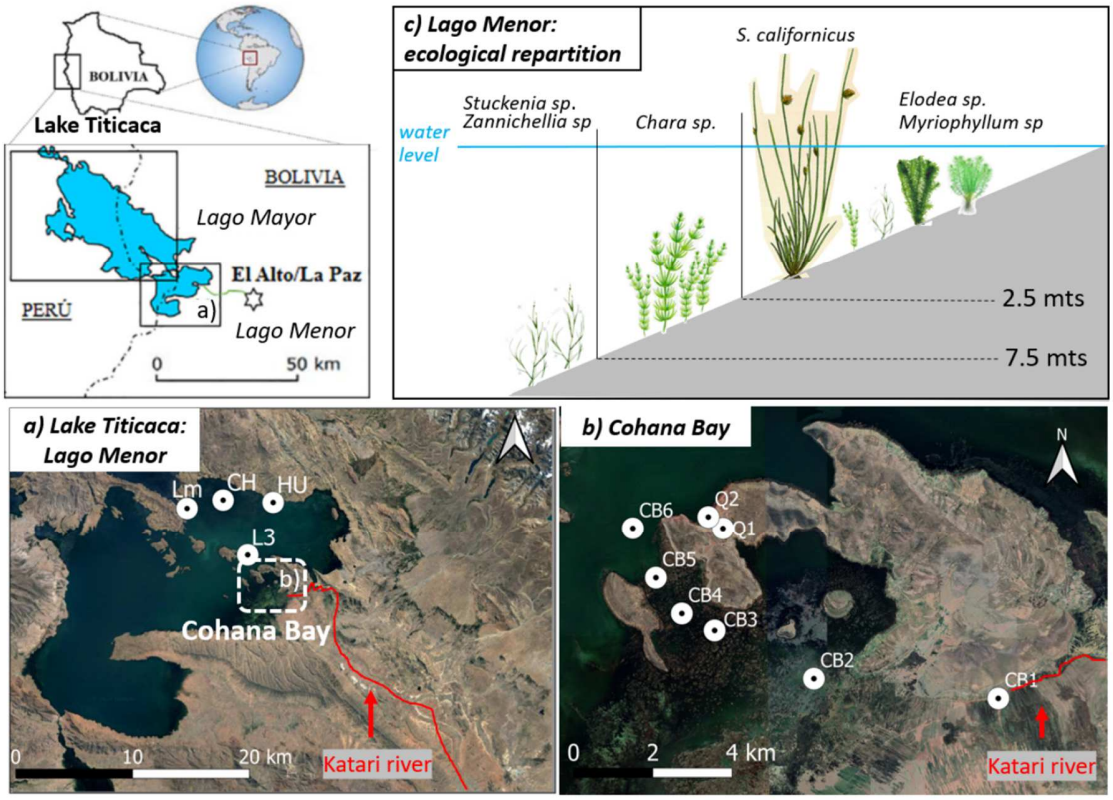

Figure 1. *Map of Lake Titicaca, presenting the sampling site location of a) control points in the coastal (CH = Chua, HU = Huatajata) and deep open waters (Lm and L3) of Lago Menor; b) the kilometric sampling points performed as a transect in the eutrophicated area of Cohana from the Katari River outlet (CB 1) to the open lake (CB 6) and from the weakly eutrophic Bay of Quehuaya (Q1 and Q2) for comparison and c) ecological repartition of the aquatic vegetation in Cohana Bay.*

This is the case for the Katari River, located in the southwestern part of Lake Titicaca, which exhibits water discharges up to 151 $m^3.s^{-1}$ during flood event, whereas its average annual discharge is 5.8 $m^3.s^{-1}$ (SENAMHI, 2020). The river drains a catchment area of more than 484

105 km^2, and is supplied by two perennial tributaries, i.e., Rio Seco (slope ~ 0.9%) and Rio Pallina
106 (slope ~ 0.03%) and many ephemeral tributaries (Chudnoff, 2009). In its upstream part, the
107 two perennial tributaries receive both treated and untreated wastewaters incoming from
108 upstream cities [i.e., El Alto City (1.2 million habitants) and Viacha (80,000 habitants)]
109 (Chudnoff, 2009; Archundia et al., 2017). Downstream, the Katari river drains a flat
110 agricultural areas where at least 65 % of the population is dedicated to agricultural and
111 livestock practices (Flores Avilés et al., 2022). Currently, only small amounts of inorganic
112 fertilizers are used in agricultural pratices (Martınez Gonzales et al., 2004; Aguilera et al., 2013).
113 The Katari River flows into the Cohana Bay (**Fig. 1b**), a large (> 86 km^2) and shallow area
114 (average depth ~ 3 m) located in the southwestern part of the southern basin of Lake Titicaca.
115 In the Bay, sediments are covered with totoras (*Schoenoplectus californicus*) in the inner margin (0-
116 2 m depth) and by macrophytes (mostly *Characeae spp.*) in the photic zones (i.e., ~ 15 m depth)
117 with maximum development between the depths of 4.5 and 7.5 m (**Fig. 1c**) (Collot et al., 1983;
118 Dejoux and Iltis, 1991).

119 *2.2. Sampling location and sample conditioning*

120 Sampling was carried out in both April and September 2013, at the end of the wet and dry
121 seasons, respectively. Six sampling sites were chosen within the Cohana Bay, starting from the
122 confluence of the Katari River (KR) in the lake, and continuing towards the interior of the lake
123 (CB 1 to CB 10.6) (**Fig. 1c**).

124 Sites were chosen following a eutrophication gradient previously determined by surface
125 concentrations of dissolved organic carbon (DOC, **Fig. 2**). Two sampling zones outside
126 Cohana Bay were chosen for comparison: i) the upper adjacent Bay of Quehuaya (Q1 and Q2)
127 and Huatajata (HU) as representative of coastal sites exhibiting a weak eutrophication, and ii)

three remote sites considered as non-impacted by anthropogenic activities: Chua (CH), the center of the open lake (L3) and just downstream of the Strait of Tiquina (Lm) which represents the water of the Lago Mayor (**Fig. 1a**).

All samples were obtained wearing nitrile gloves and collected in 50 ml polypropylene Falcon tubes to avoid cross-contamination. Macrophytes were collected manually or by dredging for the deep submerged ones. Five species belonging to four families were collected: Schoenoplectus californicus (Cyperaceae), Myriophyllum sp. (Haloagaceae), Elodea sp. (Hydrocharitaceae), Chara sp. (Characeae), and Stuckenia sp., Zannichellia sp. (Potamogetonaceae). Periphyton were collected manually by scraping them from the surface of substrate macrophytes. A Van Dorn bottle allowed the collection of water samples for SPM, then sieved and filtrated through pre-combusted glass microfiber filters (Whatman ®, GF/F, 47 mm diameter, 0.7 μm mesh). Surface sediments were collected using a gravity corer.

Samples of macrophytes, periphyton, sediments (wet season only) and suspended particulate matter (SPM, dry season only) were collected at each site, except for the Chua, L3 and Lm sites where only POM was collected. Samples of superficial soil directly upstream of the Katari River inlet were also collected. All samples were stored at -20 °C and freeze-dried before laboratory analyses.

2.3. Chemical Analysis

Physicochemical parameters (pH, redox potential, conductivity, dissolved oxygen, etc…) of the water column at each site were measured with a HANNA HI-9828 submersible multiparameter probe (Hanna Instruments, Woonsocket, RI, USA).

149 Major anions concentrations were determined by ion chromatography (Dionex ICS 2000) and
150 hydrogen sulfides by HPLC-UV following published procedures (Achá et al., 2018; Guedron
151 et al., 2020).

152 Dissolved Organic Carbon (DOC) concentrations were determined by a Non-Dispersive
153 Infra-Red (NDIR) CO_2 Shimadzu® (Model VCSN) spectrometer after humid oxidation in a
154 sodium persulfate solution at 100 °C at the geochemistry-mineralogy platform of ISTerre
155 (Grenoble, France).

156 Cavity Ring-Down Spectrometry (Picarro, Inc.®) coupled with Combustion Module (Costech,
157 Inc.®) (CM-CRDS) allowed determination of $\delta^{13}C_{bulk}$ of SPM as well as $\delta^{13}C_{org}$ of macrophytes,
158 soils and sediments at the geochemistry-mineralogy platform of ISTerre of the University
159 Grenoble-Alpes. Samples were calibrated against IAEA-603 standard. Analytical methods,
160 calibration, and sample preparation (including decarbonatation) are detailed elsewhere [Paul et
161 al. (2007, Balslev-Chausen et al. (2013, Cossa et al. (2021].

162 $\delta^{15}N$ of macrophytes, periphyton, SPM and sediment were measured using a Delta V Plus
163 continuous flow isotope ratio mass spectrometer (CF-IRMS) (Thermo Scientific, Brême,
164 Germany) with a ConFlo IV universal interface and ZeroBlank autosampler (Costech, Milan,
165 Italy), after a complete combustion of samples on a Flash EA1112 Elemental Analyzer (EA)
166 (Thermo Scientific, Milan, Italy) at the LIENSs laboratory of the University of La Rochelle
167 (France). Samples were calibrated against IAEA-N1, -N2 and -N3 standards.

168 The analytical precision was ± 0.11 ‰ (n = 27) for nitrogen (N_2) and ± 0.18 ‰ (n = 21) for
169 carbon (CO_2). The isotopic composition was reported in relation to international standards for
170 carbon (Vienna Pee Dee Belemnite - VPDB) and nitrogen (air) respectively. The data were

171 expressed according to the deviation in parts per thousand (‰) from the respective standards,
172 following the notation for isotopic composition (δ).

173 *2.4. Statistical Analysis*

174 Statistical analyses were performed using SigmaPlot version 12.5. *P* values (p) and correlation
175 coefficients (R) are reported for linear regression analyses. In all cases, a *p*-value of 0.05 was
176 chosen to indicate statistical significance.

177 **3. Results and discussions**

178

179 3.1. Natural mitigation of anthropogenic wastewater discharge in the Cohana Bay

180 Physicochemical parameters along the Cohana Bay towards the open lake are presented in
181 **Figure 2**. The highest values of pH, conductivity (up to 1000 μS cm^{-1}), and total dissolved
182 solids (TDS; up to 500 ppm) are found in the deepest part of the open Lake (i.e., Chua), which
183 is consistent with its reported relatively saline and alkaline waters (Dejoux and Iltis, 1991) that
184 result from the erosion of sulfate-rich minerals from the catchment (Banks et al., 2004; Ramos
185 Ramos et al., 2014). Dissolved oxygen content is also near oxygen saturation at both sites due
186 to the daily mixing of the water column (Dejoux and Iltis, 1991). Similar values observed in
187 the coastal site of Huatajata supports that these sites can be considered a weakly impacted area.

188

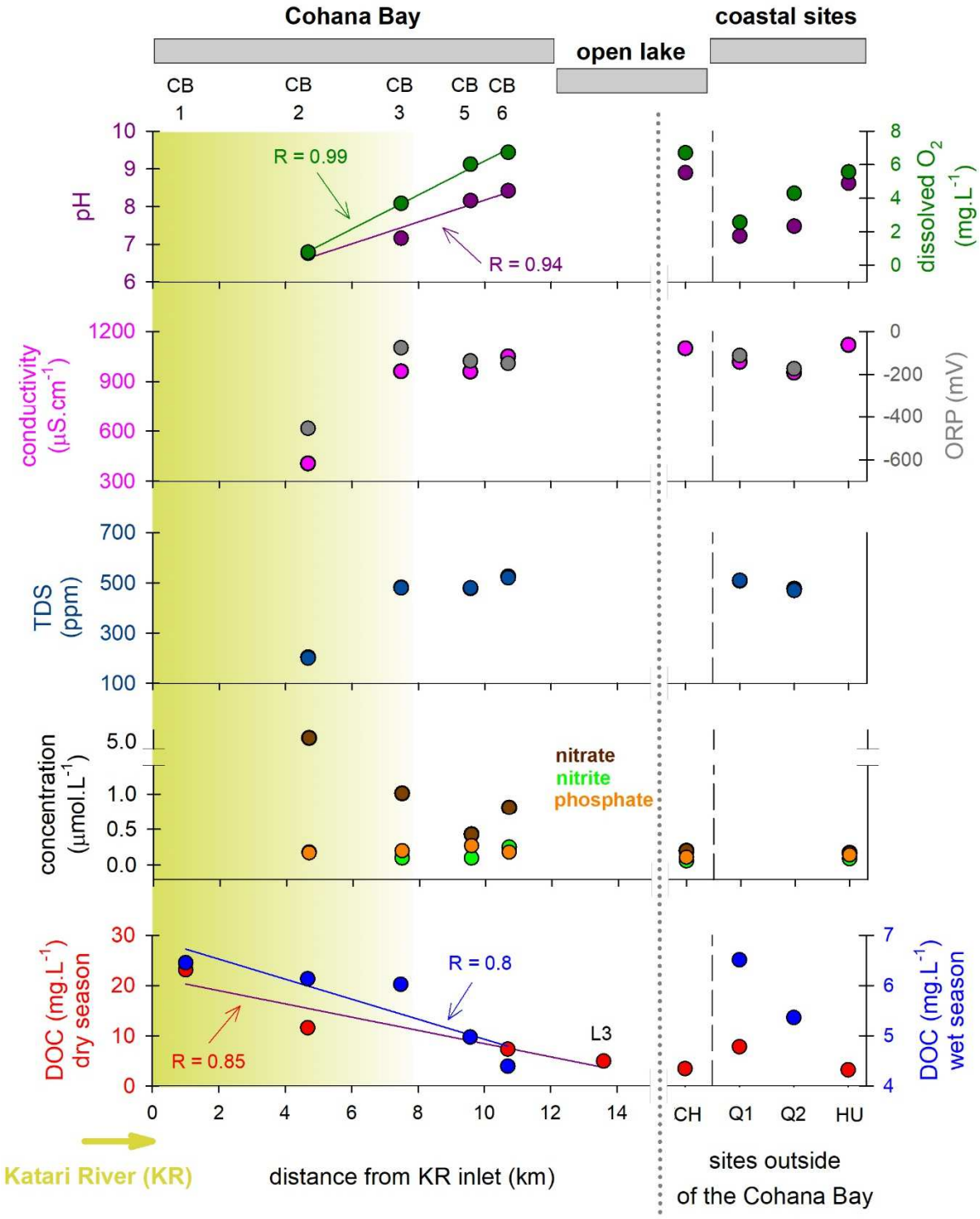

189

190 **Figure 2.** *Physicochemical parameters in surface water (1.5 meters deep) of Cohana Bay (CB 1 to CB 6), the open lake*
191 *(CH=Chua) and coastal sites (HU=Huatajata, Q1 and Q2 = Bay of Quehuaya) measured in April 2013. DOC was measured*
192 *in April (wet season) and September (dry season) 2013. Regressions are plotted only for p values < 0.05. The colored area represents*

193 *the wastewater input from the Katari River (KR). The three comparative sampling zones are indicated on the top of the figure with*
194 *gray bands.*

195

196 In contrast to the open lake, the physicochemical parameters of Cohana Bay's surface waters
197 depict major gradients along the transect, illustrating the change in water quality between the
198 inlet of the Katari river and the open lake. Previous publications (Archundia et al., 2017a;
199 Archundia et al., 2017b) have documented the quality of the Katari River network, showing
200 that water arriving at the lake had high DOC and nutrient contents but low dissolved oxygen
201 and slightly acidic to neutral pH. The physicochemical dataset obtained downstream the
202 confluence of the Katari River (i.e., CB1 and CB 2), confirms the significant contribution of
203 urban (i.e., El Alto City and Viacha City) and agricultural areas in the discharges of DOC to the
204 downstream freshwater ecosystem, a common feature of human-impacted watersheds [Stanley
205 et al. (2012), Aitkenhead-Peterson et al. (2009)]. Higher DOC concentrations were found in
206 this area during the dry season compared to the wet one (e.g. 23.1 and 6.5 mg L^{-1} at CB 2 for
207 the dry and wet season, respectively, **Fig. 2**), which illustrates the dilution of DOC in
208 wastewater during the wet season (December to April).

209 High concentration of DOC (and its organic acids) produces water acidification (Kortelainen,
210 1999) and the depletion of dissolved oxygen (Lindell et al., 1995) as observed in the first 5 km
211 downstream the Katari River inlet. Strikingly, DOC concentrations decreased gradually along
212 the transect in parallel with the rise in pH, conductivity, TDS, and dissolved oxygen from the
213 Katari River inlet site (CB 2) to the interior of the bay (CB 6). Hence, this illustrates the
214 attenuation of eutrophication within the Cohana Bay, where the water quality changes from
215 anoxic, highly reducing and moderately acidic in the first kilometers from the inlet (CB 2), to

oxic and alkaline but still reducing waters at 7.4 km (CB 3), and finally reaching similar quality status as the open lake (i.e., HU and CH) at 10.7 km (CB 6). In contrast, nitrate (NO_3^-) concentrations decreased within the first 5 km (from 5.2 to 0.8 µmol L^{-1}) whereas no variation in nitrite (NO_2^-, average = 0.13 ± 0.07 µmol L^{-1}) nor phosphate (PO_4^{3-}, average = 0.18 ± 0.05 µmol L^{-1}) were observed along the bay. Based on the annual average Katari river discharge of 5.8 $m^3.s^{-1}$ (SENAMHI, 2020), and average nitrate (3.3 ± 2.1 $mg.L^{-1}$) and phosphate (5.6 ± 3.1 $mg.L^{-1}$) concentrations in the lower Katari catchment (Archundia et al., 2017; Sarret et al., 2019); the annual nitrate and phosphate discharge to the bay are 0.6 ± 0.4 $Mg.y^{-1}$ and 1.0 ± 0.6 $Mg.y^{-1}$. The low concentrations in nutrients at CB 2 are consistent with those reported by Achá et al. (2018) for the Cohana area, but at least three times lower for NO_3^- and more than 600 times lower for PO_4^{3-} concentrations reported in the Katari River mouth (Duwig et al., 2014). This points towards a rapid assimilation of nutrients (especially phosphate) in just a few kilometers within the lake. The low concentration of nutrients along Cohana Bay, despite the anthropogenic contribution, is a clear indication of its rapid assimilation by microorganisms and algae, especially by the macrophyte-related periphyton, most of which is attached to *S. californicus* (totora) in the belts that this macrophyte forms inside the Cohana Bay.

The great capacity of nutrient absorption by periphyton has already been documented in previous studies in this bay (Sarret et al., 2019; Quiroga-Flores et al., 2021). Hence, the natural mitigation of this anthropogenic contamination in the Cohana Bay results from (i) the uptake of DOC and nutrient by aquatic vegetation and algae and (ii) its dilution with pristine freshwater from the center lake region.

In the coastal site of Bay of Quehuaya, an analog of Cohana Bay without wastewater discharge, water physicochemistry had intermediate values, similar to those found at CB 3. Such

239 moderate eutrophication status is likely due to the low-intensity anthropogenic activities in the
240 surrounding villages (i.e., domestic wastewater, subsistence livestock farming and agriculture).

241 3.2. Carbon and nitrogen isotopic composition of Lake Titicaca's ecological compartments

242 3.2.1. Macrophytes: indicators of ecotopes and anthropogenic impact

243 Aquatic plant distribution in Lake Titicaca has previously been described to depend on water
244 column depth (**Fig. 1c**). About 60 % of the Lago Menor's surface bottom is covered by
245 aquatic vegetation (Collot et al., 1983).

246 Along the Cohana Bay transect, $\delta^{13}C_{org}$ values of macrophytes (all species considered) rise with
247 the distance to the source along the eutrophication gradient (**Fig. 3**, top panel). The most
248 depleted values are in the very shallow areas near the Katari River outlet (CB 1; $\delta^{13}C_{org}$ = -29.0
249 ± 0.4 ‰ and -26.5 ± 0.2 ‰ for the wet and dry season, respectively) in the range of reported
250 values for emerged macrophytes [$\delta^{13}C_{org}$ = -26 ‰ to -28 ‰, green-colored band in **Fig. 3**,
251 Rowe et al. (2002), Miller et al. (2010)]. The highest ones are in deeper areas towards the open
252 lake (CB 6; $\delta^{13}C_{org}$ = -7.5 ± 0.6 ‰ and -8.2 ‰ for the wet and dry season, respectively), typical
253 of the range reported for submerged macrophytes (ca. -12 ± 4 ‰, **Fig. 3**, dark cyan colored
254 band) of Lake Titicaca [Rowe et al. (2002), Miller et al. (2010), Guedron et al. (2020)]. Such
255 patterns of $\delta^{13}C_{org}$ in macrophytes reflect the pathway of carbon uptake, which is related to the
256 plant's ecological distribution with water depth (e.g., emerged vs. submerged macrophytes), as
257 well as changes in the quality (trophic status) of the water column. In the very shallow coastal
258 sites, the dense vegetation of emerged macrophytes (i.e., *S. californicus*) which belongs to the
259 group of the helophytes, exhibit isotopic values (average: -26.4 ± 1.5 ‰) within the range of
260 terrestrial plants (-32 to -22 ‰), because most of the carbon is captured from the atmosphere
261 (i.e., CO_2; $\delta^{13}C$ = -8 ‰) by the leaves. In contrast, submerged macrophytes (i.e., *Myriophyllum*

262 *sp.*, *Elodea sp.*, *Chara sp.*, *Stuckenia sp.* and *Zannichellia sp.*) exhibit more positive $\delta^{13}C_{org}$ values
263 (average: -13.21 ± 6.5 ‰) because the carbon source mainly originates from the dissolved
264 inorganic carbon (DIC), which includes dissolved CO_2 and all its pH-dependent forms. Hence,
265 the difference in $\delta^{13}C_{org}$ between these aquatic plants is mostly attributable to their inorganic
266 carbon source. The boundary layer diffusion effects during atmospheric vs. aquatic
267 photosynthesis decrease the discrimination against the heavy isotope, resulting in higher $\delta^{13}C_{org}$
268 values in submerged macrophytes (Finlay and Kendall, 2007).

269

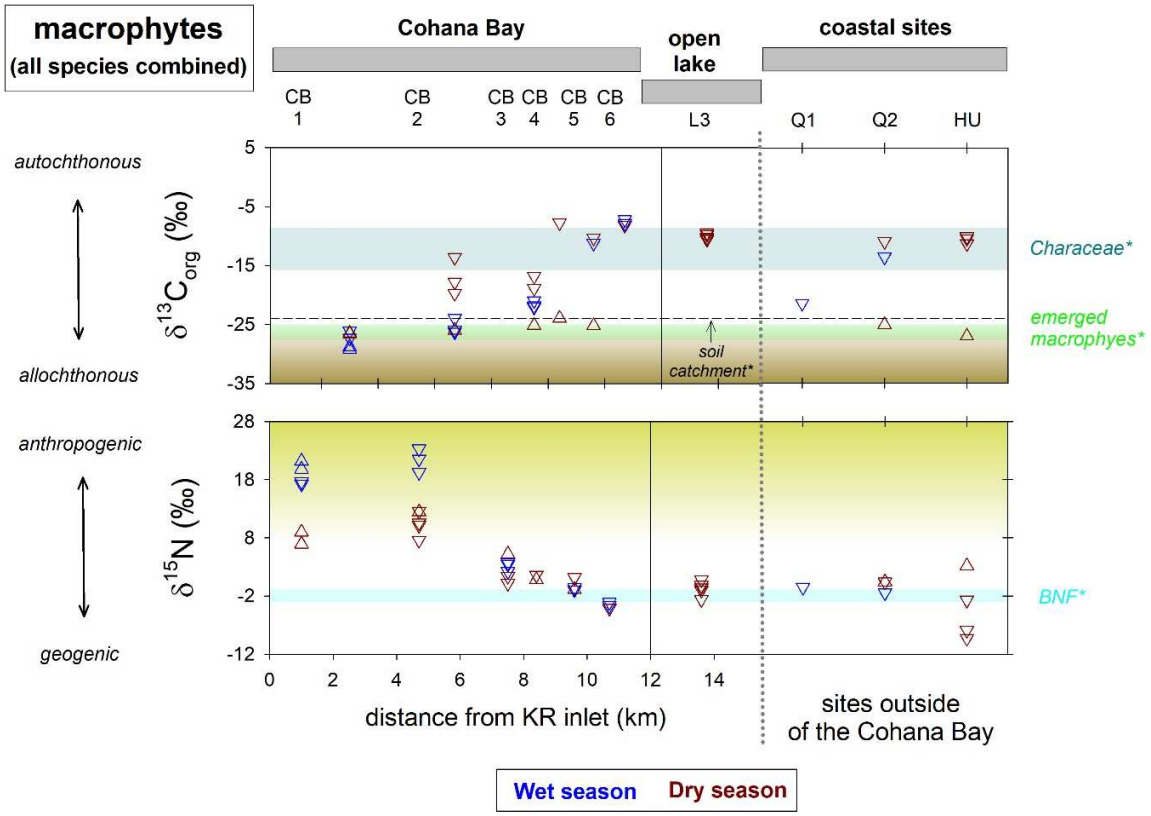

270

271 **Figure 3.** *$\delta^{13}C_{org}$ (top) and $\delta^{15}N$ (bottom) stable isotope composition of macrophytes (submerged: ▽, emerged: △) at Cohana Bay,*
272 *the open lake and coastal sites (Q1 and Q2 = Bay of Quehuaya, HU=Huatajata). Colored triangles refer to wet (blue) and dry*
273 *(red) season. Colored areas refer to: allochthonous terrestrial $\delta^{13}C$ (brown), anthropogenic $\delta^{15}N$ (yellow), submerged macrophyte $\delta^{13}C$*
274 *from lake shallows (dark cyan), emerged macrophyte $\delta^{13}C$ (green) and biological nitrogen fixation (BNF, cyan). Reference thresholds*

of colored areas are as follows: allochthonous $\delta^{13}C$ [-23 ‰, Finlay and Kendall (2007) and Chappuis et al. (2017)], anthropogenic $\delta^{15}N$ [+10 ‰, McClelland et al. (1997) and Finlay and Kendall (2007)], typical submerged macrophyte $\delta^{13}C$ [-8 to -16 ‰, Rowe et al. (2002)], typical emerged macrophyte $\delta^{13}C$ [-26 to -28 ‰, Rowe et al. (2002)] and BNF [-1 to -3 ‰, Zhang et al. (2014)]. $\delta^{13}C$ of the soil catchment (-23.8 ‰) is presented as a black dotted line. The three comparative sampling zones are indicated on the top of the figure with gray bands.

Amongst the species present in the Bay, emerged macrophytes (*S. californicus*) show similar $\delta^{13}C_{org}$ values (average: -26.4 ± 1.5 ‰) regardless of their location and the season. In contrast, submerged macrophytes collected in the coastal (Q2 and HU) and deep sites near the open lake (CB 6 and L3) exhibited the highest $\delta^{13}C_{org}$ values, up to -7 ‰ (Fig. 3). Along the Cohana bay, $\delta^{13}C_{org}$ of the submerged macrophytes decrease with distance to the KR inlet (-27.4 ± 1.3 ‰ at CB 1 to -7.7 ± 0.5 ‰ at CB 6, seasonal average) likely resulting from changing sources in the DIC pool. In submerged macrophytes near the Katari River inlet, $\delta^{13}C_{org}$ values are similar to allochthonous inputs dominated by terrestrial organic matter (OM) from the catchment (ca. -23.8 ‰, dotted line, **Fig. 3**). This indicates that the source of DIC for submerged macrophytes close to the Katari mouth mainly originates from the recycling of mixed terrestrial or anthropogenic OM. In contrast, toward the open lake, it rather originates from locally produced carbonate dissolution and the decomposition of OM, mostly from *Characeae* [-8 to -16 ‰, Rowe et al. (2002), Miller et al. (2010)].

Strikingly, nitrogen stable isotopes signatures of macrophytes exhibit a reverse trend compared to C isotopes, with decreasing $\delta^{15}N$ values with distance. . The highest $\delta^{15}N$ values are found in the very shallow areas near the Katari River outlet, with higher values during the wet season, i.e., between CB 1 ($\delta^{15}N_{wet}$ = +19.8 ± 1.8 ‰, $\delta^{15}N_{dry}$ = +8.9 ± 1.5 ‰) and CB 2 ($\delta^{15}N_{wet}$ = +21.4 ± 2.0 ‰, $\delta^{15}N_{dry}$ = +10.7 ± 2.0 ‰) which are typical of N-enriched systems [i.e.,

between +10 and +20 ‰ (McClelland, Valiela et al. 1997), dark yellow band in **Fig. 3**]. The lowest $\delta^{15}N$ values are found towards the open lake and remains in a narrow range independent of the season (e.g., CB 10.7: $\delta^{15}N$ = -3.6 ‰ ± 0.5 ‰, seasonal average), similar to those reported by Miller et al. (2010), typical of N-depleted ecosystems [-1 to -3 ‰, cyan colored band; Zhang et al. (2014]. The costal sites (Q1 = -0.51 ‰, Q2 = -0.2 ± 1.2 ‰, Hu = -4.2 ± 5.6 ‰), and relatively deep (L3 = -0.7 ± 1.1 ‰) sites show similar low values.

In contrast to carbon cycling and isotopic signature ($\delta^{13}C_{org}$), the differences in the signature of $\delta^{15}N$ between macrophytes is caused by a wide and combined range of factors, including the various metabolic pathways used for nitrogen assimilation, changes in the types of nitrogen assimilated, and the relative activity of nitrogen-fixing and denitrifying bacteria (Handley and Raven, 1992). Amongst these factors, the abundance of assimilated dissolved inorganic nitrogen (DIN) by plants, which can be in the form of nitrate (NO_3^-) and ammonium (NH_4^+), mainly depends on three major sources of supply; (i) the atmosphere (dry deposition and biological fixation), (ii) the catchment (i.e., mineralization of the OM), and (iii) fertilizers, animal or human waste (Finlay and Kendall, 2007).

In N-enriched ecosystems (e.g, human impacted environments), elevated $\delta^{15}N$ values (+10 to +20 ‰) are generally attributed to the removal of volatilized ammonia from human and animal wastes during early stages of wastewater degradation (McClelland et al., 1997) as well as the higher trophic level from which they have originated [i.e., consumers exhibit a 2 to 3 ‰ $\delta^{15}N$ enrichment relative to their diet, Kendall et al. (2007)]. In contrast, in N-limited ecosystems such as the open lake, nitrogen biological fixation (NBF) plays a major role in supplying bioavailable nitrogen (i.e., NH_3) to the N pool with $\delta^{15}N$ ratios [-1 to -3 ‰, Zhang et al. (2014)] that are close to those of atmospheric N_2 (ca. 0 ‰). (Chappuis et al., 2017).

322 The low N concentration in the entire Lake supports the hypothesis of a rapid N assimilation
323 in the water column despite the high anthropogenic discharge into the Cohana Bay, and
324 confirms that N and P are limiting factors for aquatic biota within the lake [**Fig. 2,** and Dejoux
325 and Iltis (1991**)**]. In N limited ecosystem, N uptake is expected to produce little net
326 fractionation between the $\delta^{15}N$ of DIN and macrophyte (Finlay and Kendall, 2007). Therefore,
327 $\delta^{15}N$ of macrophyte in Lake Titicaca likely integers the isotopic signature of the DIN source
328 during the plant's life cycle. Although one cannot rule out significant fractionation of N
329 associated with *in situ* growth and respiration (e.g., nitrification and denitrification) in the
330 anoxic Katari river and the Cohana bay waters and sediment, high $\delta^{15}N$ values in macrophytes
331 at the mouth of the Katari River (up to +21‰, **Fig. 3**) supports manure piles and septic waste
332 as the main anthropogenic N source. These values are consistent with $\delta^{15}N_{NO3-}$ values
333 reported for the lower Katari basin surface and ground waters (Flores Avilés et al., 2022).
334 Hence, $\delta^{15}N$ values in macrophytes confirms physico-chemical observations (Fig. 2) and
335 support anthropogenic inputs as the dominant N source within the first 5 km of the Cohana
336 Bay, whereas depleted $\delta^{15}N$ values outside this area support the fixation of atmospheric N as
337 the major supplier to the DIN pool.

338 In addition, the large seasonal variations in $\delta^{15}N$ observed within the first 5 km of the Cohana
339 Bay reflect enhanced anthropogenic N inputs during the wet season, likely resulting from the
340 leaching of urban and agricultural areas (Achá et al., 2018). In contrast, lower values $\delta^{15}N$
341 values in macrophytes at the mouth of the Katari River (+8.0 to 10.7 ‰, Fig. 3) during the dry
342 season indicates an anthropogenic contribution mixed with a depleted ^{15}N source.

343 3.2.2. Periphyton: an integrator of macrophytes and water column signal

Periphyton is defined as a biofilm composed of an assemblage of organisms (e.g., algae, bacteria, fungi, microinvertebrates, prokaryotes, and protozoa), and organic and inorganic detritus held in a mucopolysaccharide matrix attached to macrophytes (Lowe, 1996). Several studies performed in Lakes Titicaca and Uru-Uru reported the periphyton to act as a trap for suspended solids and dissolved elements, including nutrients (Alanoca et al., 2016; Lanza et al., 2017; Sarret et al., 2019; Guédron et al., 2020; Quiroga-Flores et al., 2021).

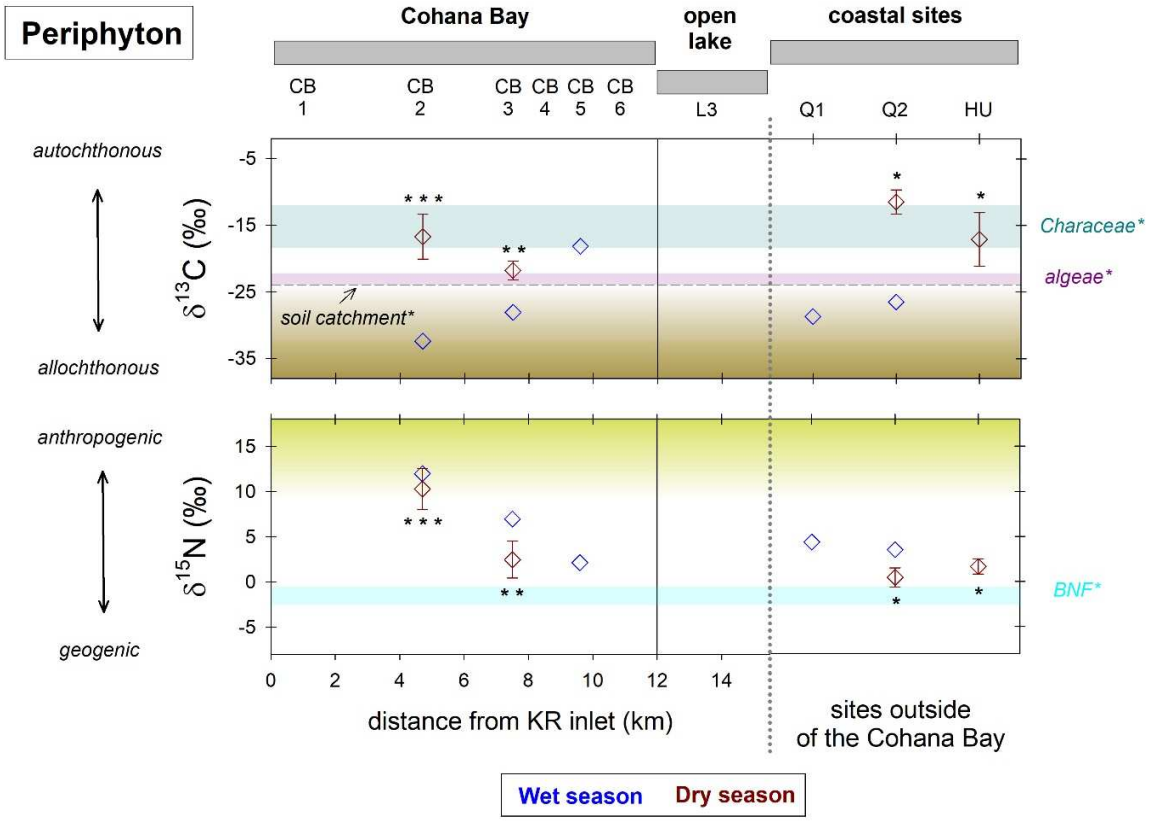

Figure 4. *$\delta^{13}C_{bulk}$ (top) and $\delta^{15}N$ (bottom) stable isotope composition of periphyton at Cohana Bay, the open lake and coastal sites (Q1 and Q2 = Bay of Quehuaya, HU=Huatajata). Colored diamonds refer to wet (blue) and dry (red) season. Error bars represent confidence intervals for data at each site. Colored areas refer to: allochthonous terrestrial $\delta^{13}C$ (brown), anthropogenic $\delta^{15}N$ (yellow), submerged macrophyte $\delta^{13}C$ from Lake Titicaca shallows (dark cyan), algae $\delta^{13}C$ (pink) and biological nitrogen fixation (BNF, cyan). Reference thresholds of colored areas are as follows: allochthonous $\delta^{13}C$ [-23 ‰, Finlay and Kendall (2007) and Chappuis et al. (2017)], anthropogenic $\delta^{15}N$ [+10 ‰, McClelland et al. (1997) and Finlay and Kendall (2007)], typical submerged*

357 *macrophyte $\delta^{13}C$ [-8 to -16 ‰, Rowe et al. (2002)], local planktonic $\delta^{13}C$ [-22.5 ‰, Rowe et al. (2002)] and BNF [-1 to -3 ‰,*
358 *Zhang et al. (2013)]. $\delta^{13}C$ of the soil catchment (-23.8 ‰) is presented as a black dotted line. The three comparative sampling zones*
359 *are indicated on the top of the figure with gray bands. The star symbols (*) indicate the hosting macrophytes from which periphyton was*
360 *taken (*: Chara sp.; **: Elodea sp. - Stuckenia sp. – Zannichellia sp.; ***: S. californicus – Stuckenia sp. –*
361 *Zannichellia sp.).*
362
363 In the entire set of periphyton samples (**Fig. 4**, top), $\delta^{13}C_{bulk}$ did not exhibit any specific spatial
364 distribution trend during the dry season, whereas a gradual increase of $\delta^{13}C$ values with
365 distance was observed in the Cohana Bay during the wet season from CB 2 ($\delta^{13}C_{bulk}$ = -32.4
366 ‰) to CB 5 ($\delta^{13}C_{bulk}$ = -18.15 ‰). It is worth mentioning that samples collected during the wet
367 season were exclusively associated with emerged macrophytes (i.e., *S. californicus)*, whereas the
368 ones collected during the dry season were associated with different macrophytes (**Fig. 4**). A
369 previous study in shallow eutrophic lakes has reported that the $\delta^{13}C$ of the periphyton closely
370 reflects the isotopic composition of the macrophyte that serves as substrate (De Kluijver et al.,
371 2015). Accordingly, the high seasonal variation at coastal site Q2 (11.3 ‰) confirms this effect,
372 where the ^{13}C-depleted value measured during the wet season is similar to that of the hosting
373 macrophyte *S. californicus*, whereas the ^{13}C-enriched value measured during the dry season
374 matches that of the submerged macrophytes (ca. -12 ± 4 ‰, dark cyan colored band in **Fig. 4**).

375 In the case of Cohana Bay, the lowest $\delta^{13}C_{bulk}$ values (average: -26.2 ± 5.4 ‰) were measured
376 during the wet season and had similar values to those of the ^{13}C-depleted OM of emerged
377 macrophytes, suggesting that the periphyton collected in the vicinity of the Katari outlet during
378 the wet season have assimilated dominantly the OM of its hosting emerged macrophyte
379 together with a contribution of entrapped or adsorbed allochthonous OM from the Katari
380 River inlet. In contrast, periphyton collected towards the open lake (i.e., CB 5) and in Huatajata

(HU) have assimilated the ^{13}C-enriched OM of the submerged macrophytes (ca. -12 ± 4 ‰, dark cyan colored band in **Fig. 4**) and algae [ca. -22.5 ‰, pink-colored band in **Fig. 4**; Rowe et al. (2002]. The higher seasonal differences found for the shallow coastal sites at CB 2 (15.7 ‰) compared to that of CB 3 (6.3 ‰) supports a significant contribution of allochthonous OM during the wet season, which decreased with distance to the Katari outlet.

In contrast to $\delta^{13}C$ signatures, the $\delta^{15}N$ of periphyton exhibited a trend similar to their hosting macrophytes, with decreasing values from +12 ‰ at CB 2 to +2.1 ‰ at CB 5 during the wet season (10 ‰ difference) and from +10.3 ± 2.3 ‰ at CB 2 to +2.5 ± 2 ‰ at CB 3 during the dry season (7.8 ‰ difference, bottom panel in **Fig. 4**). Such ca. 7.8 ‰ drop in $\delta^{15}N$ in almost 3 km confirms the rapid assimilation of the anthropogenically-derived N followed by a dominance of DIN supplied by BNF. Amongst coastal sites, Huatajata exhibited $\delta^{15}N$ ratios (+1.7 ± 0.8 ‰) typical of pristine or weakly polluted waters, whereas Bay of Quehuaya showed slightly higher $\delta^{15}N$ values (Q1 = 4.4 ‰, Q2 = 3.5 ‰) that could be attributed to a slight contribution of animal waste N inputs during the wet season.

3.2.3. Suspended particulate matter (SPM) and sediment: spatio-temporal indicators

Lake suspended particulate matter (SPM) is composed of both autochthonous (i.e., debris of primary producers and periphyton) and allochthonous organic matter (i.e., terrestrial OM from the catchment) that settles to the bottom sediment. Therefore, both the SPM and sediment can be considered as an integrative picture of the lake productivity at short and longer temporal scale, respectively.

Similar to macrophytes, $\delta^{13}C_{bulk}$ values for SPM exhibited a linear increase with distance to the KR in the Cohana Bay of 11.2 ‰ (upper panel in **Fig. 5**). However, these values remained

403 constant in the open lake and the coastal sites (average $\delta^{13}C_{bulk}$ = -17.7 ± 0.8 ‰ and -19.8 ± 0.9
404 ‰, for SPM and sediment respectively), and within the range of submerged macrophytes.
405 These observations support our earlier findings that the contribution of allochthonous and
406 anthropogenic OM inputs are significant within the eight first km within the bay. They also
407 imply a major anthropogenic OM contribution from upstream cities as the low $\delta^{13}C_{bulk}$ ratios
408 found for SPM at CB1 (-29‰) is typical of sewage effluents and catchment runoff [average
409 $\delta^{13}C_{org}$ = -24.2 ‰, Gearing et al. (1991), Rosenmeier et al. (2004)]. Further in the bay and at
410 other coastal sites, the decomposition of OM from submerged macrophytes (i.e., mostly Chara
411 sp.) is the largest supplier to the DIC pool with a small contribution from pelagic primary
412 productivity (i.e., algae).

413 Similar to SPM, $\delta^{13}C_{org}$ of sediment exhibit a gradual increase of 8.6 ‰ within the bay.
414 However, whereas the SPM exhibit very negative values close to the KR outlet, the ones of
415 sediment are in the typical range of soil and emerged macrophyte values and do not allow
416 attributing a significant anthropogenic contribution. Then, the gradual rise of $\delta^{13}C_{org}$ within the
417 bay can be attributed to the gradual change in dominant vegetation from emerged to
418 submerged macrophytes. It is worth mentioning that collected sediments covered the ten first
419 centimeters and have likely integrated the last 20 to 100 years of sedimentation. Indeed, the
420 average sedimentation rate ranges between 0.1 to 0.5 cm per year in the coastal sites of Lake
421 Titicaca (Guedron et al., 2020). Hence, the measured $\delta^{13}C_{org}$ signature integrates both the
422 historical sediment signature and possible historical change in ecological distribution related to
423 past lake-level changes (Guedron et al., 2021).

424

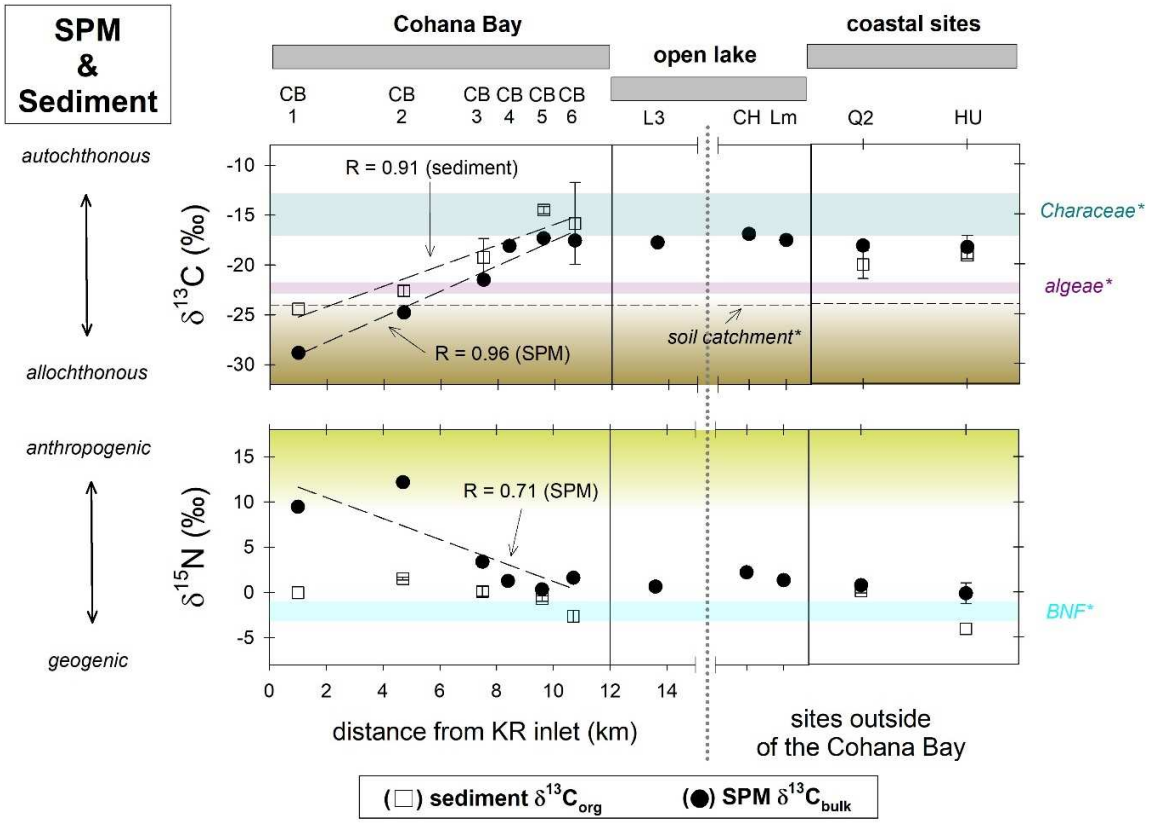

425

426 **Figure 5**. *$\delta^{13}C$ (top) and $\delta^{15}N$ (bottom) stable isotope composition of SPM (●, dry season) and sediment (□) at each sampling*
427 *site for Cohana Bay, the open lake (CH = Chua, Lm = Lago mayor) and coastal sites (Q1 and Q2 = Bay of Quehuaya,*
428 *HU=Huatajata). Error bars represent confidence intervals for data at each site. Regressions are plotted only for p values < 0.05.*
429 *Colored areas refer to: allochthonous terrestrial $\delta^{13}C$ (brown), anthropogenic $\delta^{15}N$ (yellow), submerged macrophyte $\delta^{13}C$ from Lake*
430 *Titicaca shallows (dark cyan), algae $\delta^{13}C$ (pink) and biological nitrogen fixation (BNF, cyan). Reference thresholds of colored areas*
431 *are as follow: allochthonous $\delta^{13}C$ [-23 ‰, Finlay and Kendall (2007) and Chappuis et al. (2017)], anthropogenic $\delta^{15}N$ [+10 ‰,*
432 *McClelland et al. (1997) and Finlay and Kendall (2007)], typically submerged macrophyte $\delta^{13}C$ [-8 to -16 ‰, Rowe et al.*
433 *(2002)], local planktonic $\delta^{13}C$ [-22.5 ‰, Rowe et al. (2002)] and BNF [-1 to -3 ‰, Zhang et al. (2013)]. $\delta^{13}C$ of the soil*
434 *catchment (-23.8 ‰) is presented as a black dotted line. The three comparative sampling zones are indicated on the top of the figure*
435 *with gray bands.*

436

437 The $\delta^{15}N$ values of SPM also mirrored those of macrophytes, showing a linear decrease (11.1
438 ‰ difference between CB 1 and CB 6) with increasing distance to the Katari river. As for $\delta^{13}C$,

439 the signatures of $\delta^{15}N$ remained constant in the open lake and at the coastal sites with depleted
440 values (average: $\delta^{15}N_{SPM}$ = +1 ± 1.2 ‰). Again, these $\delta^{15}N$ values close to 0 in remote areas
441 are indicative of nitrogen biological fixation [-1 to -3 ‰, **Fig. 5**, cyan colored band; Zhang et
442 al. (2014)], most likely due to insufficient NO_3^- in the DIN pool (Gu et al., 2006), contrasting
443 with values near the Katari River outlet ($\delta^{15}N$; CB 1 = +9.5 ‰, CB 2 = 12.2 ‰) where
444 wastewater-derived N is the main source.

445 In contrast, $\delta^{15}N$ values of the sediment did not show significant changes within the Cohana
446 Bay, and remained in a narrow range of variation (2.6 ‰ difference) within the range of values
447 of the BNF domain ($\delta^{15}N$ = -1.3 ± 2.4 ‰) as for the open lake and the coastal areas. Such a
448 different trend found in $\delta^{15}N$ between SPM and sediment likely results, as for $\delta^{13}C_{org}$, from the
449 large time period covered by the collected sediment cores. Hence, the recent anthropogenic
450 signal has likely been smoothed or obliterated by the pristine historical signal of the sediment.

451 3.2.4. Fingerprinting anthropogenic contamination with $\delta^{13}C$ vs $\delta^{15}N$

452 The spatial changes in both $\delta^{13}C$ and $\delta^{15}N$ signatures for macrophytes, SPM, and to a lesser
453 extent for periphyton within the Cohana Bay, reveal that anthropogenic contamination is
454 progressively attenuated within the bay. In contrast, other coastal sites (i.e., Quehuaya Bay and
455 Huatajata) distant from the Katari Outlet only show a low contamination signal.

456 At the seasonal scale, both the macrophyte and periphyton show increased spreading of the
457 anthropogenic contamination within the bay during the wet season, a period of enhanced
458 catchment leaching (i.e., soils and urban area), river discharge, and transfer of dissolved and
459 particulate C and N to the Lake. In addition, the significant inter-seasonal lake-level changes,
460 up to 2 meters (SENAMHI, 2021), also affect the ecotope distribution and the development of

specific plant species aggregates more or less tolerant to high nutrient loads depending on the season and eutrophication status.

When using 2D isotopic graphs (**Fig. 6**), the differences are clearly noticeable for the spatial changes between $\delta^{13}C$ and $\delta^{15}N$ signatures within each compartment. Indeed, the absence of a significant correlation between $\delta^{13}C$ and $\delta^{15}N$ suggests that carbon and nitrogen recycling processes are significantly different inside the bay. Regardless of the season, the $\delta^{13}C$ of macrophytes (except *S. californicus*), periphyton and SPM within the first 8 Km (i.e., between CB 3 and CB 4) exhibit lower values (**Fig. 6**) typical of allochthonous C [Finlay and Kendall (2007), Chappuis et al. (2017)].

In contrast, the $\delta^{15}N$ of the four lake compartments depict a clearer pattern of $\delta^{15}N$ depletion from anthropogenic $\delta^{15}N$-enriched values, to lower ones typical of N-biological fixation and/or atmospheric deposition around 5 km (**Fig. 6**). This rapid, close to the source, depletion of heavier N isotopes likely indicates a rapid consumption of anthropogenic N in this N-limited aquatic system, whereas the larger extension of the anthropogenic ^{13}C signal supports slower incorporation of anthropogenic C in the oligotrophic part of the system.

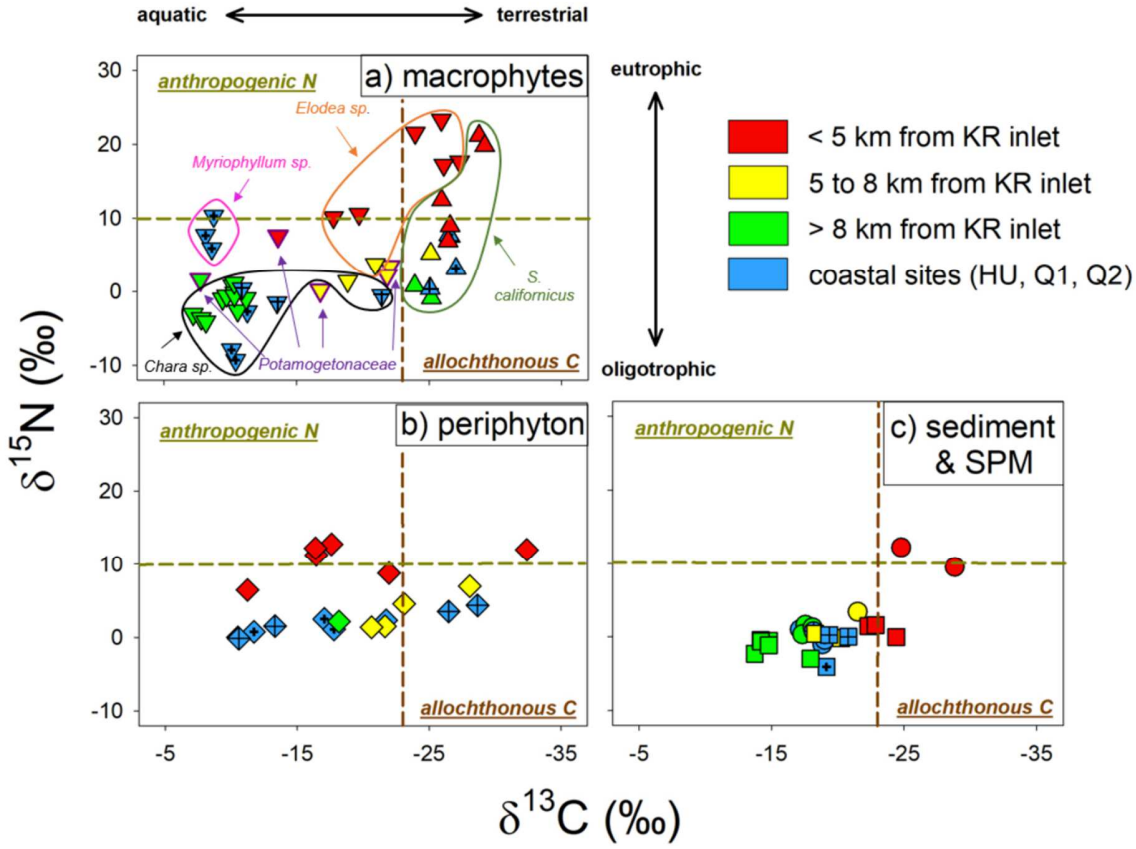

Figure 6. *$\delta^{13}C$ vs $\delta^{15}N$ biplots of: a) macrophytes (submerged: ▽, emerged: △), b) periphyton (◇), c) sediments and particulate organic matter (□ and ○, respectively) for Cohana Bay and the coastal sites (Huatajata and Bay of Quehuaya). Symbols represent individual values of each sample evaluated in this study. Colors refer to: the coastal sites (blue) and the polluted (red), transitioning (yellow) and pristine or weakly polluted areas (green) within Cohana Bay. Huatajata and Bay of Quehuaya are presented as x-hair and crossed symbols, respectively. Colored dotted lines refer to: allochthonous terrestrial $\delta^{13}C$ (brown) and anthropogenic $\delta^{15}N$ (dark yellow). Reference thresholds of colored areas are as follows: allochthonous $\delta^{13}C$ [-23 ‰, Finlay and Kendall (2007) and Chappuis, Serin□ d□ et al. (2017)] and anthropogenic $\delta^{15}N$ [+10 ‰, McClelland, Valiela et al. (1997) and Finlay and Kendall (2007)].*

Hence, three zones can be identified in the Cohana Bay: (i) the first 5 km to the Katari River outlet where anthropogenic C and N inputs dominate, (ii) a transition zone between 7 and 8

488 Km from the KR outlet that marks the mixing and dilution of urban and terrestrial OM, and
489 (iii) a pristine zone in the deepest part of the bay dominated by N-fixation and autochthonous
490 C similar to the rest of the open lake, providing the biogeochemical isotopic baseline signature
491 of the ecosystem. The larger attenuation occurs within the belt of totoras which acts as a
492 physical barrier where the biological pump (dominated by periphyton) consumes the
493 discharged nutrients and entraps floating SPM.

494 Moreover, the 3 studied compartments showed substantial differences along the
495 eutrophication gradient. Submerged macrophytes and SPM accurately illustrated the dilution
496 between anthropogenic and natural OM sources. SPM illustrates greatly the two distinct
497 anthropogenic and pristine pools, with few intermediates. For macrophytes, the ecological
498 distribution along the bay shows the distinct ability of aquatic plant species to integrate the C
499 signal depending on the plant type, water depth and quality. Indeed, whereas the emerged
500 macrophyte (i.e., S. californicus, only found in very shallow areas) does not allow the C source
501 identification because of its terrestrial-like behavior (i.e., atmospheric C incorporation), the
502 submerged macrophytes, like Chara sp. and Elodea sp., which are relatively well distributed
503 along the transect, provide a large range of $\delta^{13}C_{org}$. This is not the case for myriophyllum sp.,
504 which is only encountered in the pristine coastal site and may indicate its sensitivity to
505 eutrophication. In contrast, both macrophytes (emerged and submerged) exhibit high
506 differences in $\delta^{15}N$ signatures as they integer DIN via the aqueous media.

507 Periphyton C and N isotope signatures range in between the ones of macrophytes and SPM.
508 Their $\delta^{13}C$ values are however tightly related with those of their hosting plant (**Figs. 6a and**
509 **6b**), whereas their $\delta^{15}N$ is as narrow as the one of SPM (**Figs. 6b and 6c**) with all samples

having an atmospheric N_2 source (i.e., close to 0) except for those located within the first 5 km from the KR.

Finally, for other shallow coastal sites away from Cohana Bay (i.e., Huatajata and Bay of Quehuaya), the absence of a significant pollution signal indicated by their $\delta^{13}C$ and $\delta^{15}N$ isotopic signatures reflects their overall intact status. However, some moderately higher values indicate that agricultural land leaching is the main source of allochthonous OM during the wet season.

3.3. Significance of lake ecological compartments as bioindicators of eutrophication

3.3.1. Mixing model with $\delta^{13}C$ vs $\delta^{15}N$

To estimate the contribution of wastewater effluent as a source of C and N to the ecosystem, we used a linear mixing model to calculate plant uptake of wastewater-derived carbon and nitrogen (Cecchetti et al., 2020). In the absence of precise isotopic data for each anthropogenic source (e.g., human and animal sewage, synthetic fertilizers…), a simplified two-source linear mixing model (taking into account a natural and an anthropogenic pool) was applied to our data according to Eqs. (1) and (2) for carbon, and (3) and (4) for nitrogen:

$$\delta^{13}C_{Plants} = (\delta^{13}C_{prist}) * (f_{prist}) + (\delta^{13}C_{WW}) * (f_{WW}) \quad (1), \text{ and } 1 = f_{prist} + f_{WW} \quad (2)$$

$$\delta^{15}N_{Plants} = (\delta^{15}N_{atmos}) * (f_{atmos}) + (\delta^{15}N_{WW}) * (f_{WW}) \quad (3); \text{ and } 1 = f_{atmos} + f_{WW} \quad (4)$$

where $\delta^{13}C_{Plants}$, $\delta^{13}C_{prist}$, $\delta^{13}C_{WW}$ are the carbon isotope signatures of plants, pristine DIC and wastewater, and $\delta^{15}N_{Plants}$, $\delta^{15}N_{atmos}$, and $\delta^{15}N_{WW}$ are the nitrogen isotope signatures of plants, atmosphere and wastewater.

As mentioned previously, emerged and submerged macrophyte have different baseline $\delta^{13}C_{org}$ values because the fractionation of $^{13}C_{org}$ in macrophytes is plant-specific (i.e., pathway of DIC or atmospheric CO_2 uptake). Hence, to estimate the fraction of carbon uptaken without a single contribution of atmospheric CO_2, we only considered *Characeae* as their source of DIC may largely depend on the loading of DIC from the watershed (Bade et al., 2004), and because these submerged macrophytes have the largest distribution within the study sites. Carbon isotope endmember value for anthropogenic source ($\delta^{13}C_{WW}$) was taken from the one of SPM collected at the inlet of the Katari in Lake Titicaca (CB1; $\delta^{13}C$ = -28.8 ‰). The pristine $\delta^{13}C$-DIC reference value ($\delta^{13}C_{prist}$) was taken from average values published for $\delta^{13}C$-DIC (-8.0 ‰) at the isotopic equilibrium with the atmosphere in alkaline and slightly positive pH (~8) lakes (Bade et al., 2004), which is similar to the values found in Characeae at site CB 6 and L3, and those reported for characeae in Lake Wiñaymarca (Miller et al., 2010).

Nitrogen isotope endmember value for wastewater $\delta^{15}N$ was taken from Hydrocharitaceae samples collected during the most impacted wet season at the inlet of the KR (CB 1; $\delta^{15}N$ = 23.3 ‰) which is in the range of reported $\delta^{15}N$ for wastewater (10 to 20 ‰), and to the one of $\delta^{15}N$ in nitrate of the Katari wastewater ($\delta^{15}N$ = 19.2 ‰) from the upper part of the catchment (Flores Avilés et al., 2022). The atmospheric endmember ($\delta^{15}N_{atmos}$) was taken from the average nitrogen biological fixation (NBF = -3 ‰) reference value (Zhang et al., 2014).

The fraction of characeae biomass C contribution from wastewater to plants are represented in figure 7. Although the ^{13}C mixing model could not be applied within the first five km of the bay because of the absence of Characeae in this area, the model suggests that the wastewater contribution is still visible between seven and eight km, and in the coastal site of HU which also receives wastewater. In contrast, the anthropogenic contribution appears negligible after

554 eight km from the KR outlet as well as in the rural coastal sites of Q1 and Q2 (**Fig. 7A**). It
555 must be considered that this model is imperfect as it doesn't take into account biological
556 productivity and respiration, which could induce important changes in DIC carbon isotope
557 ratios depending on the different levels of metabolism along the slopes of the lake.

558

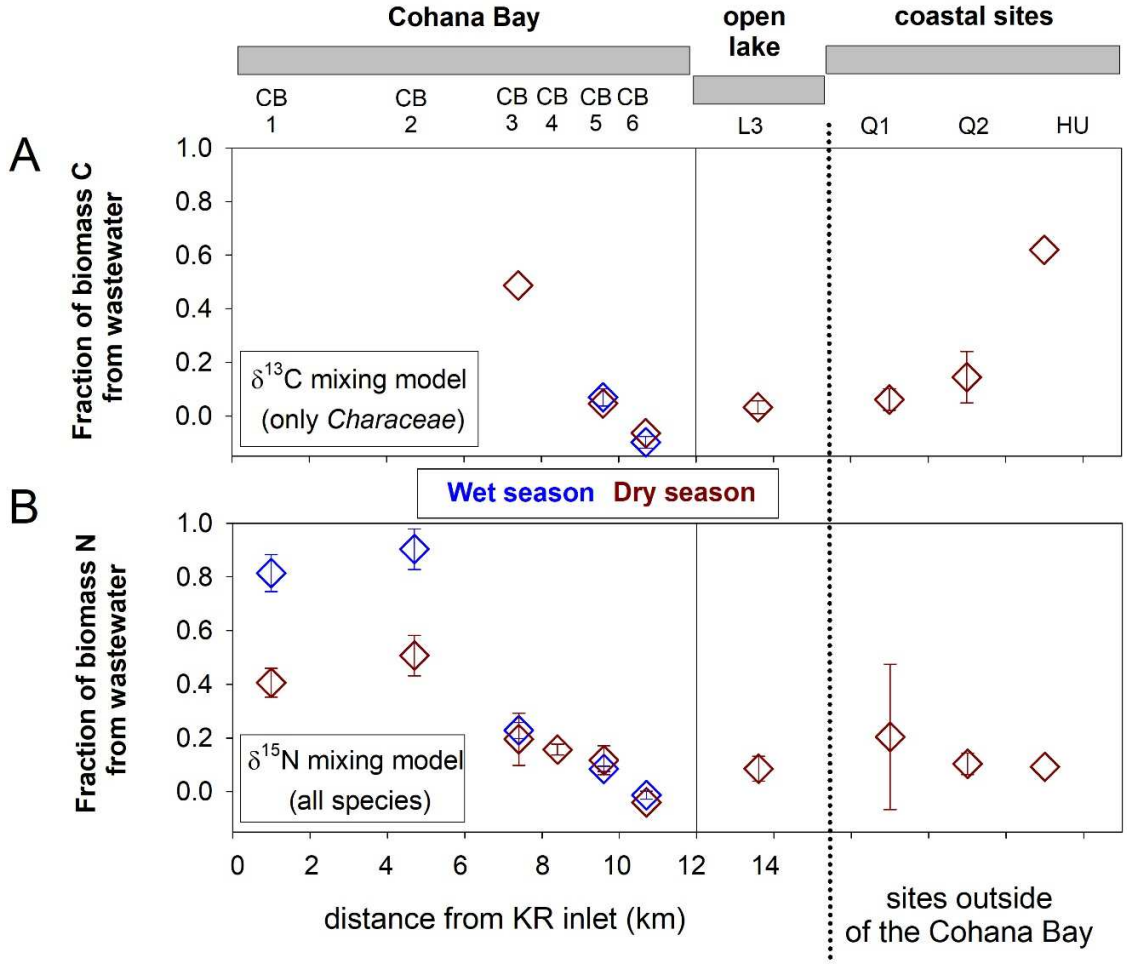

559

560 **Figure 7.** *δ^{13}Corg (top) and δ^{15}N (bottom) stable isotope mixing model of macrophytes at Cohana Bay, the open lake and coastal*
561 *sites (Q1 and Q2 = Bay of Quehuaya, HU=Huatajata). Colored diamonds refer to wet (blue) and dry (red) season. Error bars*
562 *represent confidence intervals for data at each site. The three comparative sampling zones are indicated on the top of the figure with gray*
563 *bands.*

564 The fractional contribution of biomass N from wastewater nitrogen to plants highlights a
565 gradual decrease after the first five km from the shore, where the wastewater always exceeds
566 40% to more distant areas where they drop to around 10%, even at HU. The most striking
567 feature illustrated by the model is the sharp uptake of wastewater N during the wet season
568 which reaches up to 80 % within the first 5 km of the bay, whereas it stands between 40 and
569 50% during the dry season (**Fig. 7B**).

570 **4. Conclusions and perspectives**

571

572 The study of $\delta^{13}C$ and $\delta^{15}N$ signatures within various baseline compartments of Lake Titicaca
573 show the different trophic status of the lake with areas greatly impacted by anthropogenic
574 discharges that have low $\delta^{13}C$ and high $\delta^{15}N$ signatures whereas pristine areas have high $\delta^{13}C$
575 and low $\delta^{15}N$ signatures. The gradual change in both $\delta^{13}C$ and $\delta^{15}N$ signatures along the
576 Cohana Bay transect are thus essentially driven by the change of anthropogenic and
577 background/biogeochemical natural sources. This change greatly illustrates the assimilation of
578 anthropogenically derived OM in this ecosystem, mostly attributed to the strong fixation of
579 nutrients by endemic macrophytes and their periphyton. The combined use of $\delta^{13}C$ and $\delta^{15}N$
580 brings complementary information, with $\delta^{13}C$ reporting about the C sources and recycling in
581 the ecosystem, whereas $\delta^{15}N$ provides information about the N sources and ecological
582 productivity.

583 SPM and macrophytes (except for the $\delta^{13}C$ of totoras) are the most suitable compartments for
584 tracking the dissemination of anthropogenic discharges in the lake because their $\delta^{13}C$ and $\delta^{15}N$
585 compositions accurately reflects the trophic status of the water column. The $\delta^{15}N$ signature of
586 the periphyton is also a suitable indicator of wastewater inputs, but their $\delta^{13}C$ signature shows

587 limitations due to its closeness to the $\delta^{13}C$ values of the hosting macrophyte. As a large-time
588 integrator, the sediment may also be a suitable indicator of trophic changes in the lake.

589 Hence both $\delta^{13}C$ and $\delta^{15}N$ signature in macrophytes and SPM, together with punctual physico-
590 chemical measurments indicate that anthropogenically induced eutrophication is marked within
591 the five first kilometers to the Katari river mouth, followed by a rapid attenuation or auto-
592 epuration within the next 2 to 4 km resulting from the assimilation of discharged nutrients.

593 The results presented here bring new insights that are of great interest for pollution diagnostic
594 studies and remediation strategies. For instance, filtering artificial wetlands that take advantage
595 of the periphyton capabilities as a trap of organic matter, nutrients and heavy metals can be a
596 much-needed alternative for preserving such a fragile ecosystem in front of the growing
597 human pressure.

598

599 ## Aknowledgments

600

601 This work is a contribution to the EUTITICACA project (founded by the Impuestos Directos
602 a los Hidrocarburos IDH administrated by the Universidad Mayor de San Andr_es, PI: D.
603 Acha: darioacha@yahoo.ca), COMIBOL project (INSU CNRS/IRD EC2CO Program, PI: D.
604 Point: david.point@ird.fr) and LA PACHAMAMA project (ANR CESA program, No ANR-
605 13-CESA-0015-01, PI: D. Amouroux: david.amouroux@univ-pau.fr).

606 We wish to thank, J. Gardon, A. Terrazas, C. Gonzalez, N. Clavijo, L. Salvatierra, R. Rios, J.C.
607 Salinas, A. Castillo, M. Claure, J. Tapia, J.L. Duprey (IRD Bolivia), la Familia Catari (Don
608 Ramon, Don Maximo, Don Eric, Don Ruben and Donia Maria) and Don German Calizaya

609 (Fishermen Association, Machacamarca, Bolivia) for their help and assistance during the field
610 campaigns.

611 # References

612

613 Achá D, Guédron S, Amouroux D, Point D, Lazzaro X, Fernandez PE, et al. Algal Bloom
614 Exacerbates Hydrogen Sulfide and Methylmercury Contamination in the
615 Emblematic High-Altitude Lake Titicaca. Geosciences 2018; 8: 438.
616 Aguilera J, Motavalli P, Gonzales M, Valdivia C. Response of a potato-based cropping
617 system to conventional and alternative fertilizers in the Andean highlands. Int J
618 Plant Soil Sci 2013; 3: 139-162.
619 Aitkenhead-Peterson JA, Steele MK, Nahar N, Santhy K. Dissolved organic carbon and
620 nitrogen in urban and rural watersheds of south-central Texas: land use and land
621 management influences. Biogeochemistry 2009; 96: 119-129.
622 Alanoca L, Guedron S, Amouroux D, Audry S, Monperrus M, Tessier E, et al. Synergistic
623 effects of mining and urban effluents on the level and distribution of methylmercury
624 in a shallow aquatic ecosystem of the Bolivian Altiplano. Environmental Science:
625 Processes & Impacts 2016; 18: 1550-1560.
626 Archundia D, Duwig C, Spadini L, Uzu G, Guédron S, Morel MC, et al. How Uncontrolled
627 Urban Expansion Increases the Contamination of the Titicaca Lake Basin (El Alto,
628 La Paz, Bolivia). Water, Air, & Soil Pollution 2017; 228: 44.
629 Archundia D, Duwig C, Spadini L, Uzu G, Guedron S, Morel MC, et al. How Uncontrolled
630 Urban Expansion Increases the Contamination of the Titicaca Lake Basin (El Alto,
631 La Paz, Bolivia). Water, Air, and Soil Pollution 2017a; 228: 1-17.
632 Archundia D, Duwig C, Lehembre F, Chiron S, Morel MC, Prado B, et al. Antibiotic
633 pollution in the Katari subcatchment of the Titicaca Lake: Major transformation

products and occurrence of resistance genes. Science of the Total Environment 2017b; 576: 671-682.

Backer LC, McGillicuddy Jr DJ. Harmful Algal Blooms at the Interface Between Coastal Oceanography and Human Health. Oceanography 2006; 19: 94-106.

Bade DL, Carpenter SR, Cole JJ, Hanson P, Hesslein RH. Controls of d13C-DIC in lakes: Geochemistry, lake metabolism, and morphometry. Limnology and Oceanography 2004; 49: 1160-1172.

Balslev-Chausen D, Dahl TW, Saad N, Rosing MT. Precise and accurate δ13C analysis of rock samples using flash combustion-cavity ring down laser spectroscopy. Journal of Analytical Atomic Spectrometry 2013; 28: 516-523.

Banks D, Markland H, Smith PV, Mendez C, Rodriguez J, Huerta A, et al. Distribution, salinity and pH dependence of elements in surface waters of the catchment areas of the Salars of Coipasa and Uyuni, Bolivian Altiplano. Journal of Geochemical Exploration 2004; 84: 141-166.

Cecchetti AR, Sytsma A, Stiegler AN, Dawson TE, Sedlak DL. Use of stable nitrogen isotopes to track plant uptake of nitrogen in a nature-based treatment system. Water Research X 2020; 9.

Chappuis E, Seriñá V, Martí E, Ballesteros E, Gacia E. Decrypting stable-isotope (δ13C and δ15N) variability in aquatic plants. Freshwater Biology 2017; 62: 1807-1818.

Chudnoff SM. A Water Quality Assessment of the Rio Katari River and its Principle Tributaries, Bolivia. Earth and Environmental Science. Master in water resources. The University of New Mexico, Albuquerque, New Mexico, 2009, pp. 143.

656 Cole ML, Kroeger KD, Mcclelland JW, Valiela I. Effects of Watershed Land use on
657 Nitrogen Concentrations and δ15 Nitrogen in Groundwater. Biogeochemistry 2006;
658 77: 199-215.
659 Collot D, Koriyama F, García E. Répartitions, biomasses et productions des macrophytes
660 du lac Titicaca. Revue D'hydrobiologie Tropicale 1983; 16: 241-261.
661 Cossa D, Mucci A, Guédron S, Coquery M, Radakovitch O, Escoube R, et al. Mercury
662 accumulation in the sediment of the Western Mediterranean abyssal plain: A
663 reliable archive of the late Holocene. Geochimica et Cosmochimica Acta 2021; 309:
664 1-15.
665 Costanzo SD, O'Donohue MJ, Dennison WC, Loneragan NR, Thomas M. A New
666 Approach for Detecting and Mapping Sewage Impacts. Marine Pollution Bulletin
667 2001; 42: 149-156.
668 Dawson TE, Mambelli S, Plamboeck AH, Templer PH, Tu KP. Stable isotopes in plant
669 ecology. Annual review of ecology and systematics 2002; 33: 507-559.
670 Dawson TE, Siegwolf RT. Using stable isotopes as indicators, tracers, and recorders of
671 ecological change: some context and background. Terrestrial Ecology 2007; 1: 1-18.
672 De Kluijver A, Ning J, Liu Z, Jeppesen E, Gulati R, Middelburg J. Macrophytes and
673 periphyton carbon subsidies to bacterioplankton and zooplankton in a shallow
674 eutrophic lake in tropical China. Limnology and Oceanography 2015; 60: 375-385.
675 Dejoux C, Iltis A. Lake Titicaca: A synthesis of limnological knowledge. Monographie
676 Biologicae. 68. Kluvier Academic Publisher, Dordrecht, 1991, pp. 560.
677 Diaz RJ. Overview of Hypoxia around the World. Journal of Environmental Quality 2001;
678 30: 275-281.

679 Dodds WK, Bouska WW, Eitzmann JL, Pilger TJ, Pitts KL, Riley AJ, et al. Eutrophication
680 of U.S. Freshwaters: Analysis of Potential Economic Damages. Environmental
681 Science & Technology 2009; 43: 12-19.
682 Duwig C, Archundia D, Lehembre F, Spadini L, Morel MC, Uzu G, et al. Impacts of
683 Anthropogenic Activities on the Contamination of a Sub Watershed of Lake
684 Titicaca. Are Antibiotics a Concern in the Bolivian Altiplano? Procedia Earth and
685 Planetary Science 2014; 10: 370-375.
686 Finlay JC, Kendall C. Stable isotope tracing of temporal and spatial variability in organic
687 matter sources to freshwater ecosystems. In: Michener R, Lajtha K, editors. Stable
688 isotopes in ecology and environmental science. Blackwell Publishing, 2007, pp.
689 283-333.
690 Flores Avilés GP, Spadini L, Sacchi E, Rossier Y, Savarino J, Ramos OE, et al.
691 Hydrogeochemical and nitrate isotopic evolution of a semiarid mountainous basin
692 aquifer of glacial-fluvial and paleolacustrine origin (Lake Titicaca, Bolivia): the
693 effects of natural processes and anthropogenic activities. Hydrogeology Journal
694 2022; 30: 181-201.
695 Fry B. Stable isotope ecology. Vol 521. New York, NY: Springer, 2006.
696 Gearing PJ, Gearing JN, Maughan JT, Oviatt CA. Isotopic distribution of carbon from
697 sewage sludge and eutrophication in the sediments and food web of estuarine
698 ecosystems. Environmental Science & Technology 1991; 25: 295-301.
699 Glibert PM, Middelburg JJ, McClellan JW, Vander Zanden MJ. Stable Isotope tracers:
700 Enriching our perspectives and questions on sources, fates, rates, and pathways of

major elements in aquatic systems. Limnology and Oceanography 2018; 64: 950-981.

Gu B, Chapman AD, Schelske CL. Factors controlling seasonal variations in stable isotope composition of particulate organic matter in a softwater eutrophic lake. Limnology and Oceanography 2006; 51: 2837-2848.

Guedron S, Audry S, Achá D, Bouchet S, Point D, Condom T, et al. Diagenetic production, accumulation and sediment-water exchanges of methylmercury in contrasted sediment facies of Lake Titicaca (Bolivia). Science of the Total Environment 2020; 723: 1-14.

Guedron S, Tolu J, Delaere C, Sabatier P, Barre J, Heredia C, et al. Reconstructing two millennia of copper and silver metallurgy in the Lake Titicaca region (Bolivia/Peru) using trace metals and lead isotopic composition. Anthropocene 2021; 34: 100288.

Guédron S, Point D, Acha D, Bouchet S, Baya PA, Molina CI, et al. Mercury contamination level and speciation inventory in the hydrosystem of Lake Titicaca: current status and future trends. Environmental Pollution 2017; 231: 262-270.

Guédron S, Ledru MP, Escobar-Torrez K, Develle AL, Brisset E. Enhanced mercury deposition by Amazonian orographic precipitation: Evidence from high-elevation Holocene records of the Lake Titicaca region (Bolivia). Palaeogeography, Palaeoclimatology, Palaeoecology 2018; 511: 577-587.

Guédron S, Achá D, Bouchet S, Point D, Tessier E, Heredia C, et al. Accumulation of Methylmercury in the High-Altitude Lake Uru Uru (3686 m asl, Bolivia) Controlled by Sediment Efflux and Photodegradation. Applied Sciences 2020; 10: 7936.

723 Handley LL, Raven JA. The use of natural abundance of nitrogen isotopes in plant
724 physiology and ecology. Plant, Cell and Environment 1992; 15: 965-985.
725 Holtgrieve GW, Schindler DE, Hobbs WO, Leavitt PR, Ward EJ, Bunting L, et al. A
726 Coherent Signature of Anthropogenic Nitrogen Deposition to Remote Watersheds
727 of the Northern Hemisphere. Science 2011; 334: 1545-1548.
728 Kendall C, Elliott EM, Wankel SD. Tracing Anthropogenic Inputs of Nitrogen to
729 Ecosystems. Stable Isotopes in Ecology and Environmental Science, 2007, pp. 375-
730 449.
731 Kendall C, Elliott EM, Wankel SD. Tracing Anthropogenic Inputs of Nitrogen to
732 Ecosystems. Stable Isotopes in Ecology and Environmental Science. Blackwell
733 Publishing Ltd, 2008, pp. 375-449.
734 Kortelainen P. Acidity and buffer capacity. In: Keskitalo J, Eloranta P, editors. Limnology
735 of Humic Waters. Backhuys, Leiden, 1999, pp. 95-115.
736 Lanza WG, Achá D, Point D, Masbou J, Alanoca L, Amouroux D, et al. Association of a
737 Specific Algal Group with Methylmercury Accumulation in Periphyton of a
738 Tropical High-Altitude Andean Lake. Archives of Environmental Contamination
739 and Toxicology 2017; 72: 1-10.
740 Le Moal M, Gascuel-Odoux C, Menesguen A, Souchon Y, Ettrillard C, Levain A, et al.
741 Eutrophication: A new wine in and old bottle? Science of the Total Environment
742 2018: 1-11.
743 Lindell MJ, Granéli W, Tranvik LJ. Enhanced bacterial growth in response to
744 photochemical transformation of dissolved organic matter. Limnology and
745 Oceanography 1995; 40: 195-199.

746 Liu B, Yan H, Wang C, Li Q, Guédron S, Spangenberg JE, et al. Insights into low fish
747 mercury bioaccumulation in a mercury-contaminated reservoir, Guizhou, China.
748 Environ. Poll. 2012; 160: 109-117.
749 Lowe RL. Periphyton patterns in lakes. In: Stevenson RJ, Bothwell ML, Lowe RL, editors.
750 Algal ecology freshwater benthic ecosystems. Academic Press, San Diego, 1996,
751 pp. 781.
752 Mariotti A, Landreau A, Simon B. 15N isotope biogeochemistry and natural denitrification
753 process in groundwater: application to the chalk aquifer of northern France.
754 Geochimica et Cosmochimica Acta 1988; 52: 1869-1878.
755 Martınez Gonzales I, Roncal RZ, Miranda AP, Gotilla JS. Co-Operation on the Lake
756 Titicaca. UNESCO-IHP, Paris, France, 2004.
757 Mazurek H. El censo en Bolivia, una herramienta de desarrollo. T'inkasos. 15, 2012.
758 McClelland JW, Valiela I, Michener RH. Nitrogen-stable isotope signatures in estuarine
759 food webs: A record of increasing urbanization in coastal watersheds. Limnology
760 and Oceanography 1997; 42: 930-937.
761 Michener R, Lajtha K. Stable isotopes in ecology and environmental science: John Wiley &
762 Sons, 2008.
763 Middelburg JJ. Stable isotopes dissect aquatic food webs from the top to the bottom.
764 Biogeosciences 2014; 11: 2357-2371.
765 Miller M, Capriles J, Hastorf CA. The Fish of Lake Titicaca: Implications for Archaeology
766 and Changing Ecology through Stable Isotope Analysis. Journal of Archaeological
767 Science 2010; 37: 317-327.

768 Molina J, Satge F, Pillco R. Los recursos hidricos del TDPS. In: Puilly M, Lazzaro X, Point
769 D, Aguirre M, editors. Linea Base de Conocimientos sobre los Recursos
770 Hidrologicos en el Sistema TDPS con enfoque en la cuenca del Lago Titicaca. IRD-
771 UICN, Quito, Ecuador, 2014.
772 Northcote TG. Contamination. In: Dejoux C, Iltis A, editors. Lake Titicaca: A Synthesis of
773 Limnological Knowledge. Springer Netherlands, Dordrecht, 1992, pp. 551-561.
774 Paerl HW, Otten TG. Harmful Cyanobacterial Blooms: Causes, Consequences, and
775 Controls. Microbial Ecology 2013; 65: 995-1010.
776 Paul D, Skrzypek G, Fórizs I. Normalization of measured stable isotopic compositions to
777 isotope reference scales – a review. Rapid Communications in Mass Spectrometry
778 2007; 21: 3006-3014.
779 Pretty JN, Mason CF, Nedwell DB, Hine RE, Leaf S, Dils R. Environmental Costs of
780 Freshwater Eutrophication in England and Wales. Environmental Science &
781 Technology 2003; 37: 201-208.
782 Quiroga-Flores R, Guédron S, Acha D. High methylmercury uptake by green algae in Lake
783 Titicaca: Potential implications for remediation. Ecotoxicology and Environmental
784 Safety 2021; 207: 111256.
785 Ramos Ramos O, Rotting TS, French M, Sracek O, Bundschuh J, Quintanilla J, et al.
786 Geochemical processes controlling mobilization of arsenic and trace elements in
787 shallow aquifers and surface waters in the Antequera and Poopó mining regions,
788 Bolivian Altiplano. Journal of Hydrology 2014; 518: 421-433.

789 Richerson PJ, Neale PJ, Wurstbaugh W, Alfaro R, VIncent WF. Patterns of temporal
790 variation in primary production and other limnological variables in Lake Titicaca, a
791 high-altutude torpical lake. Hydrobiologia 1986; 138: 205-220.
792 Roche MA, Bourges J, Cortes J, Mattos R. IV.1. Climatology and hydrology of the Lake
793 Titicaca basin. In: Dejoux C, Iltis A, editors. Lake Titicaca - A synthesis of
794 limnological Knowledge. 68. Kluwer Academic Publishers,
795 Dordrecht/Boston/London, 1992, pp. 63-88.
796 Rosenmeier MF, Brenner M, Kenney WF, Whitmore TJ, Taylor CM. Recent
797 Eutrophication in the Southern Basin of Lake Petén Itzá, Guatemala: Human Impact
798 on a Large Tropical Lake. Hydrobiologia 2004; 511: 161-172.
799 Rowe HD, Dunbar RB, Mucciarone DA, Seltzer GO, Baker PA, Fritz SC. Insolation,
800 moisture balance and climate change on the South American Altiplano since the
801 Last Glacial Maximum. Climatic Change 2002; 52: 175-199.
802 Sarret G, Guédron S, Acha D, Bureau S, Arnaud-Godet F, Tisserand D, et al. Extreme
803 Arsenic Bioaccumulation Factor Variability in Lake Titicaca, Bolivia. Scientific
804 Reports 2019; 9: 10626.
805 Savage C. Tracing the influence of sewage nitrogen in a coastal ecosystem using stable
806 nitrogen isotopes. AMBIO: A Journal of the Human Environment 2005; 34: 145-
807 150.
808 Schindler DE, Carpenter SR, Cole JJ, Kitchell JF, Pace ML. Influence of food web
809 structure on carbon exchange between lakes and the atmosphere. Science 1997; 277:
810 248-251.

811 Schindler DW. Recent advances in the understanding and management of eutrophication.
812 Limnology and Oceanography 2006; 51: 356-363.
813 Sebilo M, Billen G, Grably M, Mariotti A. Isotopic composition of nitrate-nitrogen as a
814 marker of riparian and benthic denitrification at the scale of the whole Seine River
815 system. Biogeochemistry 2003; 63: 35-51.
816 Segura H, Junquas C, Espinoza JC, Vuille M, Jauregui YR, Rabatel A, et al. New insights
817 into the rainfall variability in the tropical Andes on seasonal and interannual time
818 scales. Climate Dynamics 2019; 1: 1-22.
819 SENAMHI. Reporte Semanal Lago Titicaca. Abril, 2021.
820 SENAMHI B. Servicio Nacional de Meteorología de Hidrología. La Paz, Bolivia 2020;
821 http://www.senamhi.gob.bo.
822 Smith RS, King KW, Williams MR. What is causing the harmful algal blooms in Lake
823 Erie? Journal of Soil and Water Conservation 2015; 70: 27-29.
824 Smith VH. Eutrophication of freshwater and coastal marine ecosystems a global problem.
825 Environmental Science and Pollution Research 2003; 10: 126-139.
826 Smith VH, Joye SB, Howarth RW. Eutrophication of freshwater and marine ecosystems.
827 Limnology and Oceanography 2006; 51: 351-355.
828 Stanley EH, Powers SM, Lottig NR, Buffam I, Crawford JT. Contemporary changes in
829 dissolved organic carbon (DOC) in human dominated rivers: is there a role for DOC
830 management? Freshwater Biology 2012; 57: 26-42.
831 Thevenon F, Adatte T, Spangenberg JE, Anselmetti FS. Elemental (C/N ratios) and isotopic
832 ($d^{15}Norg$,$d^{13}Corg$) compositions of sedimentary organic matter from a high-altitude

mountain lake (Meidsee, 2661 m asl, Switzerland): Implications for Lateglacial and Holocene Alpine landscape evolution. The Holocene 2012; 22: 1135-1142.

Vahtera E, Conley DJ, Gustafsson BG, Kuosa H, Pitkänen H, Savchuk OP, et al. Internal Ecosystem Feedback Enhance Nitrogen-fixing Cyanobacteria Blooms and Complicate Management in the Baltic SeaA. Ambio 2007; 36: 186-194.

Vander Zanden MJ, Rasmussen JB. Primary consumer δ 13 C and δ 15 N and the trophic position of aquatic consumers. Ecology 1999: 1395-1404.

Vermeulen S, Sturaro N, Gobert S, Bouquegneau JM, Lepoint G. Potential early indicators of anthropogenically derived nutrients: a multiscale stable isotope analysis. Marine Ecology Progress Series 2011; 422: 9-22.

Villafae VE, Andrade M, Lairana V, Zaratti F, Helbling EW. Inhibition of phytoplankton photosynthesis by solar ultraviolet radiation: studies in Lake Titicaca, Bolivia. Freshwater Biology 1999; 42: 215-224.

Zhang X, Sigman DM, Morel FMM, Kraepiel AML. Nitrogen isotope fractionation by alternative nitrogenases and past ocean anoxia. Proceedings of the National Academy of Sciences of the United States 2014; 111: 4782-4787.